# Ocean acidification impacts growth and shell mineralization in juvenile abalone (*Haliotis tuberculata*)

Stéphanie Auzoux-Bordenave[1,8*], Nathalie Wessel[2], Aïcha Badou[3], Sophie Martin[4,8], Saloua M'Zoudi[5], Solène Avignon[1], Sabine Roussel[6], Sylvain Huchette[7], Philippe Dubois[5]

[1]UMR "Biologie des Organismes et Ecosystèmes Aquatiques" (BOREA), /MNHN/CNRS/ SU/IRD/, Muséum National d'Histoire Naturelle, Station Marine de Concarneau, 29900 Concarneau, France
[2]Ifremer, Département Océanographie et Dynamique des Ecosystèmes (ODE), Rue de l'île d'Yeu, BP21105, 44311 Nantes Cedex 3, France
[3]Muséum National d'Histoire Naturelle, Station Marine de Concarneau, 29900 Concarneau, France
[4]UMR 7144 "Adaptation et Diversité en Milieu Marin" (AD2M), CNRS/SU, Station Biologique de Roscoff, 29680 Roscoff Cedex, France
[5]Laboratoire de Biologie Marine, Université Libre de Bruxelles, CP160/15, 1050, Brussels, Belgium
[6]Univ Brest, CNRS, IRD, Ifremer, LEMAR, 29280 Plouzané, France
[7]Ecloserie France Haliotis, Kerazan, 29880 Plouguerneau, France
[8]Sorbonne Université (SU), 4, place Jussieu, 75005 Paris, France

* Corresponding author: tel: + 33 2 98 50 42 88; fax: + 33 2 98 97 81 24,
E-mail: stephanie.auzoux-bordenave@mnhn.fr

## Abstract

Ocean acidification is a major global driver that leads to substantial changes in seawater carbonate chemistry, with potentially serious consequences for calcifying organisms. Marine shelled molluscs are ecologically and economically important species, providing essential ecosystem services and food sources for other species. Due to their physiological characteristics and their use of calcium carbonate ($CaCO_3$) to build their shells, molluscs are among the most vulnerable invertebrates with regard to ocean acidification, with early developmental stages being particularly sensitive to pH changes. This study investigated the effects of $CO_2$-induced ocean acidification on juveniles of the European abalone *Haliotis tuberculata*, a commercially important gastropod species. Six-month-old juvenile abalones were cultured for 3 months at four pH levels (8.1, 7.8, 7.7, 7.6) representing current and predicted near-future conditions. Survival, growth, shell microstructure, thickness and strength were compared across the four pH treatments. After three months of exposure, significant reductions in juvenile shell length, weight and strength were revealed in the pH 7.6

treatment. SEM observations also revealed modified texture and porosity of the shell mineral layers as well as alterations of the periostracum at pH 7.6 which was the only treatment with an aragonite saturation state below 1. It is concluded that low pH induces both general effects on growth mechanisms and corrosion of deposited shell in *H. tuberculata*. This will impact both the ecological role of this species and the costs of its aquaculture.

**Keywords:** ocean acidification; abalone; juvenile; growth; shell mineralization

## Introduction

Anthropogenic carbon dioxide emission and its subsequent absorption by the ocean is responsible for seawater pH decrease and reduced availability of carbonate ions, leading to a decrease of calcium carbonate saturation state, two processes known as ocean acidification (OA) (Doney et al. 2009; Gattuso et al. 2015; IPPC 2014). Future projections suggest there will be a pH reduction of 0.3 units by the year 2100, threatening marine organisms that produce calcium carbonate exoskeletons and shells, such as corals, molluscs and echinoderms (Kroeker et al. 2010; Hendricks et al. 2010; Hofmann et al. 2010; Widdicombe and Spicer 2008; Wittmann and Pörtner 2013). Because they do not compensate for acid-base disturbances, molluscs are considered to be among the most vulnerable invertebrates with respect to OA, with a pronounced sensitivity in larval and juvenile stages (Beniash et al. 2010; Gazeau et al. 2013; Melzner et al. 2009; Orr et al. 2005; Przeslawski et al. 2015, Ross et al. 2011). In marine shelled molluscs, OA has been shown to reduce larval survival, lengthen development time, alter morphology and/or impair shell formation and calcification (Byrne et al. 2011; Duquette et al. 2017; Ellis et al. 2009; Fitzer et al. 2014a; Gazeau et al. 2010; Kurihara 2008; Noisette et al. 2014). Since many mollusc species are sources of

commercially important foods, negative impacts of OA may also result in significant economic loss (Ekstrom et al. 2015; Gazeau et al. 2007).

Abalone are ecologically and economically important shelled gastropods, which are grazers in the marine ecosystem and a food delicacy for humans (Cook 2014; Huchette and Clavier 2004). Many abalone species worldwide have experienced severe population decline due to both overfishing and environmental perturbations, such as global warming and disease (Nicolas et al. 2002; Travers et al. 2009). In the context of the growth of worldwide aquaculture (Cook 2014), understanding the effects of stress on abalone physiology would allow the farmers to adapt their practices to minimize stress, prevent mortalities and produce higher quality shellfish (Morash and Alter 2015).

The abalone *Haliotis tubercula* is a commercially important species, for which rearing over the whole life cycle is controlled in aquaculture (Courtois de Viçose et al. 2007). It displays a pelago-benthic life cycle with a larval planktonic stage followed by a critical metamorphosis into the benthic juvenile, making this species highly sensitive to environmental changes (Byrne et al. 2011). Several studies have focused on early life-history stages of abalone, especially on larvae, and have demonstrated adverse effects of elevated $CO_2$, such as reduced survival, developmental delay, body and shell abnormalities and reduction in mineralization (Byrne et al. 2011; Crim et al. 2011; Guo et al. 2015; Kimura et al. 2011; Onitsuka et al. 2018; Wessel et al. 2018; Zippay and Hofmann 2010). Shell formation has been extensively studied in *H. tuberculata*, revealing that aragonite is the main $CaCO_3$ polymorph (Auzoux-Bordenave et al. 2010, 2015). Since aragonite is a less stable polymorph than calcite and is likely to be more susceptible to dissolution (Morse et al. 2007), the abalone shell is expected to be more sensitive to OA (Gazeau et al. 2013). The juvenile stage is a relevant model to study the effects of OA since (i) it corresponds to the growing stage between larvae and adults and (ii) it is a critical period where abalone are submitted to strong predation (Shepherd 1973). So far, only two studies investigated the responses of juvenile abalone to decreased

seawater pH. In juvenile *Haliotis iris* from New Zealand, significant reduction of shell growth was observed under lower pH (0.3 to 0.5 pH units less than the control), but no effect on respiration rate (Cunningham et al. 2016). More recently, the effects of low pH (- 0.3 to - 0.5 units below control pH) on juvenile *H. discus hannai* resulted in eroded shell surfaces, reduced growth rates and altered biochemical composition and energy metabolism (Li et al. 2018). The impact on shell microstructure or resistance to fracture was not investigated.

The goal of the present study was to investigate the effects of $CO_2$-induced ocean acidification on survival, growth and shell mineralization and mechanics of juveniles of the European abalone *H. tuberculata*. Six-month-old juvenile abalones were cultured for three months under current and near-future pH conditions (8.1, 7.8, 7.7 and 7.6). Biological responses such as survival rate, growth performance (shell length, weight and shell growth) and shell biomineralization were compared across the different pH treatments. SEM microscopy and fracture force analyses were performed to assess whether reduced pH has an influence on shell microstructure, thickness and resistance.

## Materials and methods

### Abalone collection and rearing

Farmed, 6-month-old juvenile abalones *H. tuberculata* (n = 540 in total, 6.0 ± 0.5 mm total shell length) were collected from nursery tanks at the France Haliotis abalone farm (48°36'46N, 4°33'30W; Plouguerneau, France) in January 2013 and transported to the laboratory at the marine station, Concarneau (MNHN, France). The abalone were randomly distributed into 12 experimental aquaria (12 L) supplied with filtered 3µm natural seawater renewed at a rate of 6 $L.h^{-1}$ and aerated with ambient air. Temperature was the local value in January, i.e., 9.3°C ± 0.5 °C. Animals were conditioned in the laboratory, at ambient $pCO_2$, at

a density of 45 abalones per aquarium, for 3 weeks. Juvenile abalone shells usually have a green coloration, resulting from their grazing on *Ulvella sp*. algae at the farm. At the start of the experiment, the abalone diet was changed from green algae *Ulvella* to red *Palmaria palmata* which is a high quality alga giving the best growth performance for *H*. *tuberculata* (Mercer et al. 1993). This changeover is part of standard procedure in aquaculture when juveniles reach 6–10 mm and results in a change of shell colouration from greenish to red (Marchais et al. 2017). Shell maerking by algal feeding can be used as a proxy to determine growth in long term stock enhancement program (Gallardo et al. 2003). This transition allowed us to mark the start (T0) of the experimental period for the evaluation of shell growth. The abalones were fed once a week *ad libitum* with the red macroalgae *Palmaria palmata*.

## Experimental design

Experiments were carried out between March and June 2013 at the Concarneau marine station (France) according to an experimental design adapted from Martin et al. (2011). Juvenile abalones were exposed to four pH levels (Total scale) for 3 months. The treatments consisted of a control at present-day pH, $pH_T$ 8.1 ($pCO_2 \approx 400$ µatm), and three levels of predicted $pH_T$ according to different climate change scenarios, as outlined in Riebesell et al. (2010): 7.8 ($pCO_2 \approx 750$ µatm), 7.7 ($pCO_2 \approx 1000$ µatm) and 7.6 ($pCO_2 \approx 1400$ µatm). Three replicate aquaria were set up per pH treatment.

## pH control and carbonate chemistry

Low seawater $pH_T$ levels were obtained by bubbling $CO_2$ (Air Liquide, France) into three 100 L header tanks supplied with filtered through-flowing seawater, continuously aerated with ambient air. Each header tank supplied three experimental 12 L aquaria at a rate of 6 $L.h^{-1}$. $pCO_2$ in each tank was regulated through electro-valves controlled by a pH-stat system (IKS Aquastar, Germany). pH values of the IKS system were adjusted from daily measurements of the electromotive force (emf) in each aquarium using a pH meter (Metrohm 826 pH mobile, Metrohm, Switzerland) with a glass electrode (Metrohm electrode plus), converted to total scale pH units ($pH_T$) using Tris/HCl and 2-aminopyridine/HCl buffers (Dickson 2010). At the start of the experiment, pH was gradually decreased over 10 days by 0.05 pH $unit.day^{-1}$ until the different target pH levels were reached.

Seawater parameters were monitored throughout the 3-month experiment. Temperature and $pH_T$ were recorded almost daily in each of the 12 experimental aquaria using a pH meter as described above. Salinity was measured twice a week using a conductivity meter (3110, WTW, Germany). Total seawater alkalinity ($A_T$) was measured every two weeks on 100 mL samples taken from each experimental aquarium. Seawater samples were filtered through 0.7 µm Whatman GF/F membranes, immediately poisoned with mercury chloride and stored in a cool dark place pending analyses. $A_T$ was determined potentiometrically using an automatic titrator (TitroLine alpha, Schott SI Analytics, Germany), calibrated with the National Bureau of Standards scale. $A_T$ was calculated using a Gran function applied to pH values ranging from 3.5 to 3.0, as described by Dickson et al. (2007), and corrected by comparison with standard reference material provided by Andrew G. Dickson (CRM Batch 111). Seawater carbonate chemistry, i.e., dissolved inorganic carbon (DIC), $pCO_2$ and aragonite saturation state ($\Omega_{aragonite}$) were calculated from $pH_T$, $A_T$, temperature and salinity with the $CO_2$SYS

161 program (Pierrot et al. 2006) using constants from Mehrbach et al. (1973) refitted by Dickson
162 and Millero (1987).
163
164 **Juvenile survival and sampling**
165
166 Survival of the juvenile abalones was assessed almost daily during the 3-month experiment.
167 Any dead individuals were removed from the tanks immediately. Mortality was calculated as
168 the proportion of the number of dead abalones vs the total number of abalones per tank and
169 then averaged over the three replicates to calculate the mean survival for each pH treatment.
170 Juvenile individuals were sampled at the start of the experiment (T0) and after 3 months of
171 exposure (T3m). Soft tissues were dissected while shells were rinsed with distilled water,
172 dried and stored at room temperature until analysis.
173
174 **Biometric measurements**
175
176 Shell length was measured with a Vernier calliper to the nearest 0.05 mm on 12 abalones
177 from each replicate (n = 36 per pH treatment). Shell dry weight was measured on an
178 analytical laboratory balance (Ohaus, Switzerland) to the nearest 0.001 mg (n = 21 per pH
179 treatment, except for pH 7.6, n = 13). For shell weight, the lower number of individuals in
180 $pH_T$ 7.6 is due to the high percentage of broken shells in this condition; indeed, only the
181 whole shells were used for shell weight determination and further SEM analysis on cross
182 sections. The remaining shell samples were used for shell strength measurements. Shell index
183 was calculated as the ratio total shell weight/(shell length)$^3$ (n = 21 per pH treatment , except
184 for pH 7.6, n = 13).
185

For the estimation of relative shell growth, the external mark on the shell induced by the change in algal diet (Fig. 1) was used as a proxy to estimate the shell area newly formed during the 3-month experiment. Shell surfaces were examined under a binocular microscope (Leica, Germany) and imaged with NIS elements software (Nikon, Japan). For the determination of relative shell growth, the newly formed area (red coloured) was measured by tracing its outline using Image J software. The ratio of red shell area/total shell area was calculated for each abalone shell and used as a proxy to determine relative shell growth (n = 36 per pH treatment). All measurements were made by a single researcher, with the origin of each shell anonymised to eliminate subjective bias.

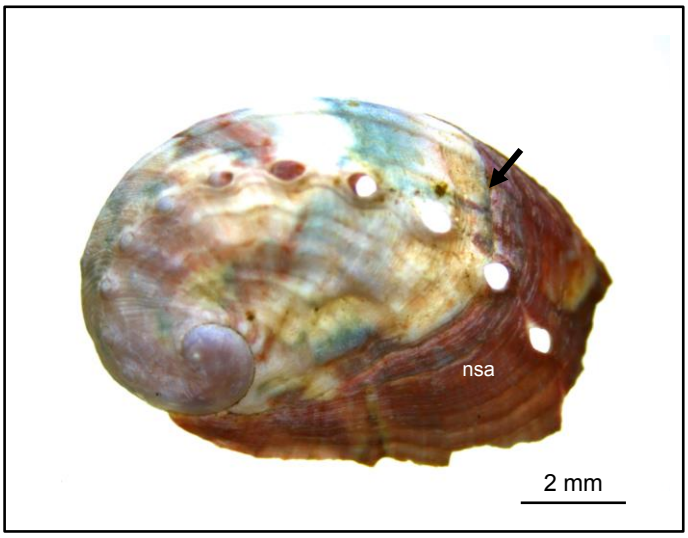


**Fig. 1** Shell of a 9-month-old abalone showing the transition from greenish to red colouration induced by the change of algal diet (black arrow); the transition mark was used as a proxy to estimate the shell area newly (nsa) formed during the 3-month experiment.

## Scanning electron microscopy (SEM)

Randomly chosen abalone shells from control pH and pH 7.6 (n = 5 per pH treatment) were analysed by SEM. Outer and inner shell surfaces were investigated on whole, gold-coated

(JEOL JFC 1200 fine coater) samples. Shell thickness and microstructure were examined on shell cross-sections cut using a razor blade along the longitudinal growth axis of the shell. Samples were gold-coated (JEOL JFC 1200 fine coater) and observed at 5–15 kV with either a JEOL JSM-840A or a Sigma 300 FE-SEM scanning electron microscope (SEM, Plateau Technique de Microscopie Electronique, MNHN, Paris and Concarneau, France). Shell thickness (total, outer spherulitic and nacre layer thickness) measurements were made on SEM images of the cross sections using Image J software from 6 to 9 transects per shell section (Fig. S1, electronic supplementary material).

## Biomechanical tests

Shell strength (resistance) of abalone shells was measured individually (n = 10 shells/pH treatment) using a simple compression method. The shells were placed on a metal block with the opening downwards (i.e., in what would be their natural position on a rocky substrate) and the mechanical test was carried out using a second metal block fixed on the load frame of the force stand (Instron 5543), which was then lowered onto the shell at a speed of 0.3 $mm.min^{-1}$ (simple compression test) until fracture. Displacement and force were recorded continuously at a frequency of 10 Hz using a 100N force cell (Instron 2530-100N). The failure force was recorded for each specimen. A representative curve of compressive force vs displacement is presented in supplementary Fig. S2. A stress-strain relationship was not established because of the absence of symmetry in the abalone shell and the difficulty to define the surface on which the force is applied.

## Statistical analysis

All statistical analyses were performed with Rstudio software (R Core Team, 2015). Differences in juvenile survival, shell length and weight, relative growth and shell index across pH treatments were assessed using generalized linear model (GLM) ANOVAs after testing the normality of data, normality of residuals and homogeneity of variances (pH: fixed factor, tank: random factor nested into pH). In the few cases where data distribution deviated from normality and/or variances were not homogeneous, data were Log-transformed to ensure compliance with ANOVA assumptions. If the homogeneity of variance was not verified, a Welch test was performed, as recommended by Day and Quinn (1989). Post-hoc HSD Tukey tests, using the appropriate mean square error, were used to test the differences between the group means. To detect any significant differences in shell thickness, unpaired Student's t-tests were performed. To assess the effect of decreased pH on shell strength, regression analyses were performed to look at the relationships between fracture force and shell weight. ANCOVA model was used to compare linear regression models and evaluate the effect of pH, using weight as a covariate. All data are presented as means ± SD, except where otherwise stated. Differences were considered significant at $P < 0.05$.

# Results

## Seawater parameters

Mean values of seawater carbonate chemistry parameters for the four pH treatments are given in Table 1. Seawater temperature followed the natural variations found in the bay of Concarneau, ranging from 9.3 ± 0.5°C at the start of experiment (early March) to 16.1 ±

0.5°C at the end (mid-June), with the mean ranging from 12.1 ± 1.8°C to 12.4 ± 1.8°C according to treatment. The $pH_T$ of the experimental aquaria was maintained close to the nominal values throughout the experiment, at $pH_T$ = 8.10 ($pCO_2$ = 347 ± 5 µatm), $pH_T$ = 7.81 ($pCO_2$ = 746 ± 10 µatm), $pH_T$ = 7.73 ($pCO_2$ = 934 ± 13µatm) and $pH_T$ = 7.65 ($pCO_2$ = 1157 ± 35 µatm). Mean total alkalinity ($A_T$) measured in the experimental aquaria ranged from 2305 ± 28 µEq.kg$^{-1}$ to 2312 ± 30 µEq.kg$^{-1}$ (n= 8 per pH treatment) over the course of the experiment and presented only slight differences between treatments. Salinity was 35.2 ± 1.7 in all experimental aquaria. $\Omega_{calcite}$ was always greater than 1 in all four pH treatments, while $\Omega_{aragonite}$ only reached values below 1 in the lowest $pH_T$ treatment (7.6).

## Survival

The mortality of juvenile abalones was very low, with a survival percentage ranging between 90.9 ± 10.3% and 96 ± 3.3% at the end of the experiment. There were no significant differences in survival among the four pH treatments (ANOVA, $F(3,8) = 0.367$, $P = 0.78$).

## Shell growth

Abalones grew in all treatments, from 6.0 ± 0.5 mm at the start of the experiment to 8.3 ± 1.0 mm ($pH_T$ 8.1), 8.7 ± 1.0 mm ($pH_T$ 7.8), 8.1 ± 1.0 mm ($pH_T$ 7.7) and 7.8 ± 1.1 mm ($pH_T$ 7.6) after 3 months. Total shell length after 3 months differed significantly according to pH treatment (ANOVA, $F(3,8) = 4.78$, $P = 0.034$, Fig. 2): juveniles exposed to $pH_T$ 7.6 were significantly smaller than those exposed to $pH_T$ 7.8 (Post-hoc Tukey, $t8 = -3.656$, $P = 0.027$, Table 2). No significant differences were observed between juveniles exposed to $pH_T$ 7.7, 7.8 and the control $pH_T$ (8.1).

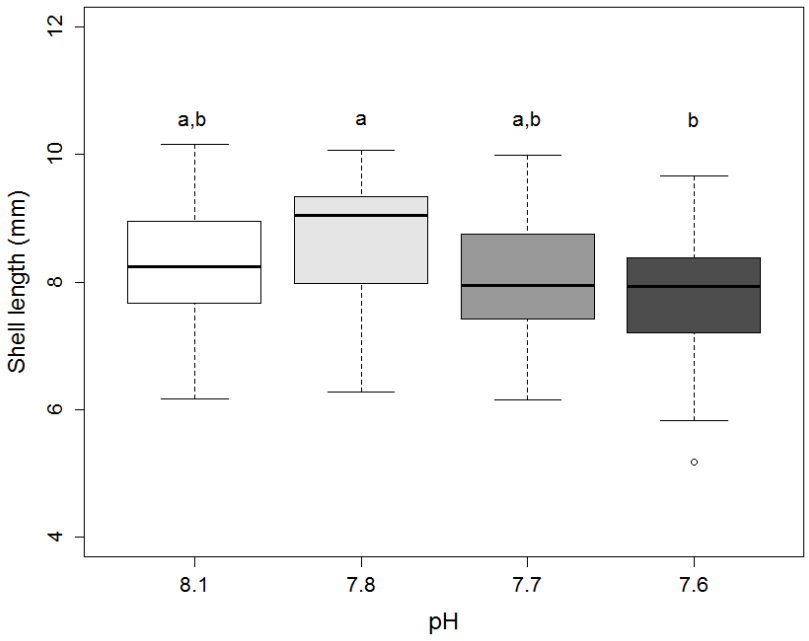


**Fig. 2** Shell length of juvenile abalones *H. tuberculata* exposed to decreased $pH_T$ values. Centre lines of box plots show the medians; box limits indicate the first and third quartiles, respectively, with whiskers encompassing data within 1.5 times the spread from the median (n = 36 per pH treatment). Different letters indicate significant differences between pH treatments ($P < 0.05$).

Shell weight was significantly affected by pH (ANOVA, $F(3,8) = 24.43$, $P < 0.001$, Fig. 3), being lower for juveniles exposed to $pH_T$ 7.6 compared with those grown in other pH treatments (Post-hoc Tukey, $P < 0.005$, Table 2). Relative shell growth, determined as the ratio of red shell area/total shell area, did not differ significantly between pH treatments (ANOVA, $F(3,8) = 0.626$, $P = 0.618$, Table 2).

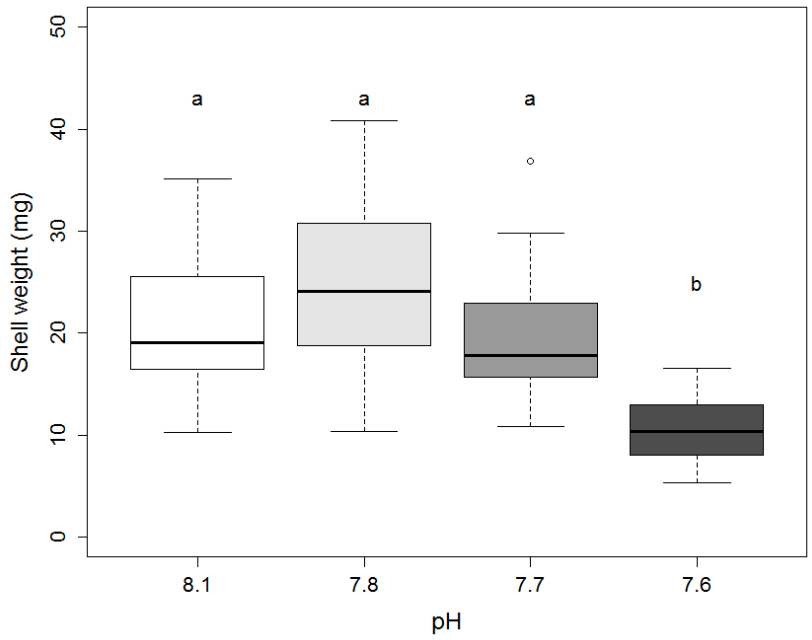


**Fig. 3** Shell weight of juvenile abalones *H. tuberculata* exposed to decreased $pH_T$ values. Centre lines of box plots show the medians; box limits indicate the first and third quartiles respectively, with whiskers encompassing data within 1.5 times the spread from the median (n = 22 per pH treatment, except for pH 7.6 n = 13). Different letters indicate significant differences between pH treatments ($P < 0.05$).

## Shell calcification

Shell index was significantly affected by pH (Welch's F-test, $F(3, 3.982) = 14.48$, $P = 0.013$; Fig. 4). Abalones in the $pH_T$ 7.6 treatment had a reduced shell index compared to those grown in the other pH treatments ($P < 0.005$, Table 2).

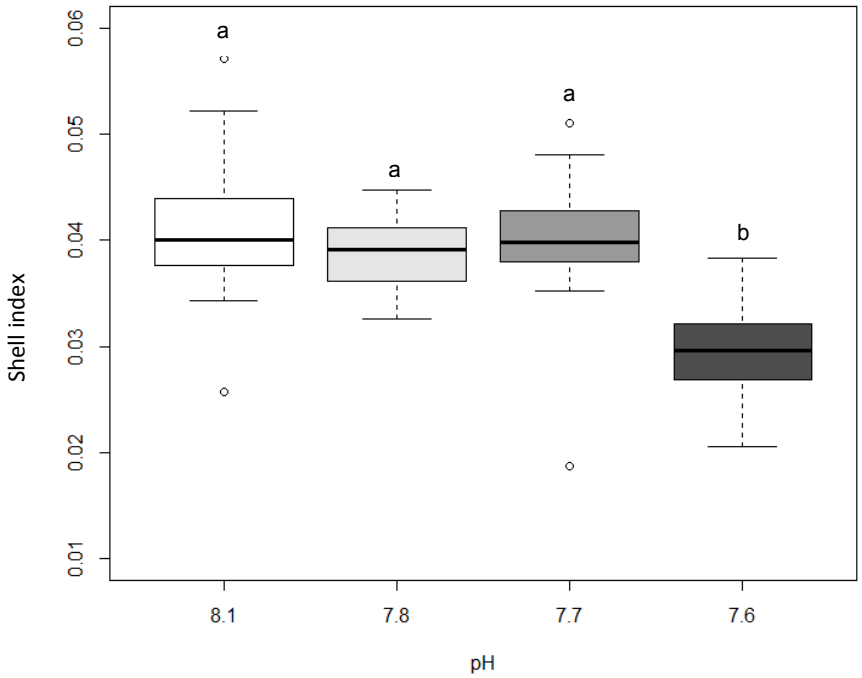


**Fig. 4** Shell index (determined as the ratio shell weight/shell length$^3$) of juvenile abalones under different $pH_T$ conditions. Centre lines of box plots show the medians; box limits indicate the first and third quartiles, respectively, with whiskers encompassing data within 1.5 times the spread from the median (n = 22 per pH treatment, except for $pH_T$ 7.6 n = 13). Different letters indicate significant differences between pH treatments ($P < 0.05$).

SEM examination of abalone shells grown at $pH_T$ 8.1 and 7.6 revealed differences in the texture and porosity of both outer and inner surface layers. Under control conditions, almost intact periostracum were observed with typical ornamentations (ridge and groove pattern)and regular organic sheets (Fig. 5a, c). At lower pH, the periostracum revealed bleached areas and a corroded surface with numerous small holes (Fig. 5b, d). In some individuals, large holes were observed between the apertures as the result of shell corrosion (Fig. 5b). The delamination of surface organic sheets revealed biominerals of the underlying spherulitic layer (Fig. 5d). In control shells, the inner nacreous layer had a homogeneous surface, with a gradual maturation of aragonite platelets (Fig. 6a, c, e). By contrast, juvenile shells from the low pH treatment (pH 7.6) were characterized by a partial degradation of the inner nacreous

355 layer, resulting in decreased size of aragonite platelets and irregularities of their edges (Fig.
356 6b, d, f).
357

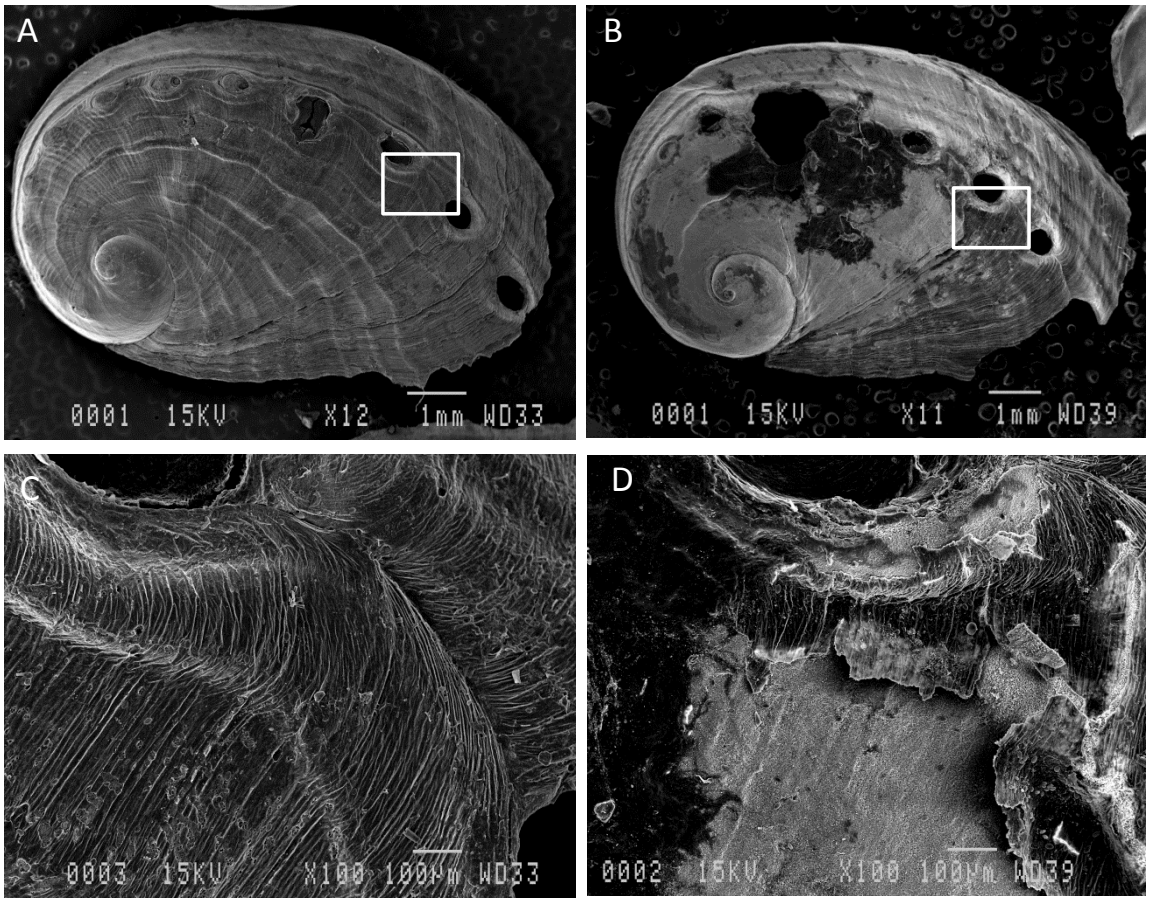


358

359 **Fig. 5** SEM images of abalone outer shell surface in control conditions ($pH_T$ 8.1: A, C) and
360 under lower pH ($pH_T$ 7.6: B, D). **A**. Periostracum in the control, showing a homogenous
361 surface with the typical ridge and groove patterns; **B**. Periostracum in the $pH_T$ 7.6 treatment,
362 showing bleached areas and corroded surface; **C.** Detail of the shell area boxed in A, showing
363 regular organic sheets; **D.** Detail of the shell area boxed in B, showing the delamination of
364 organic sheets and revealing biominerals of the underlying spherulitic layer.

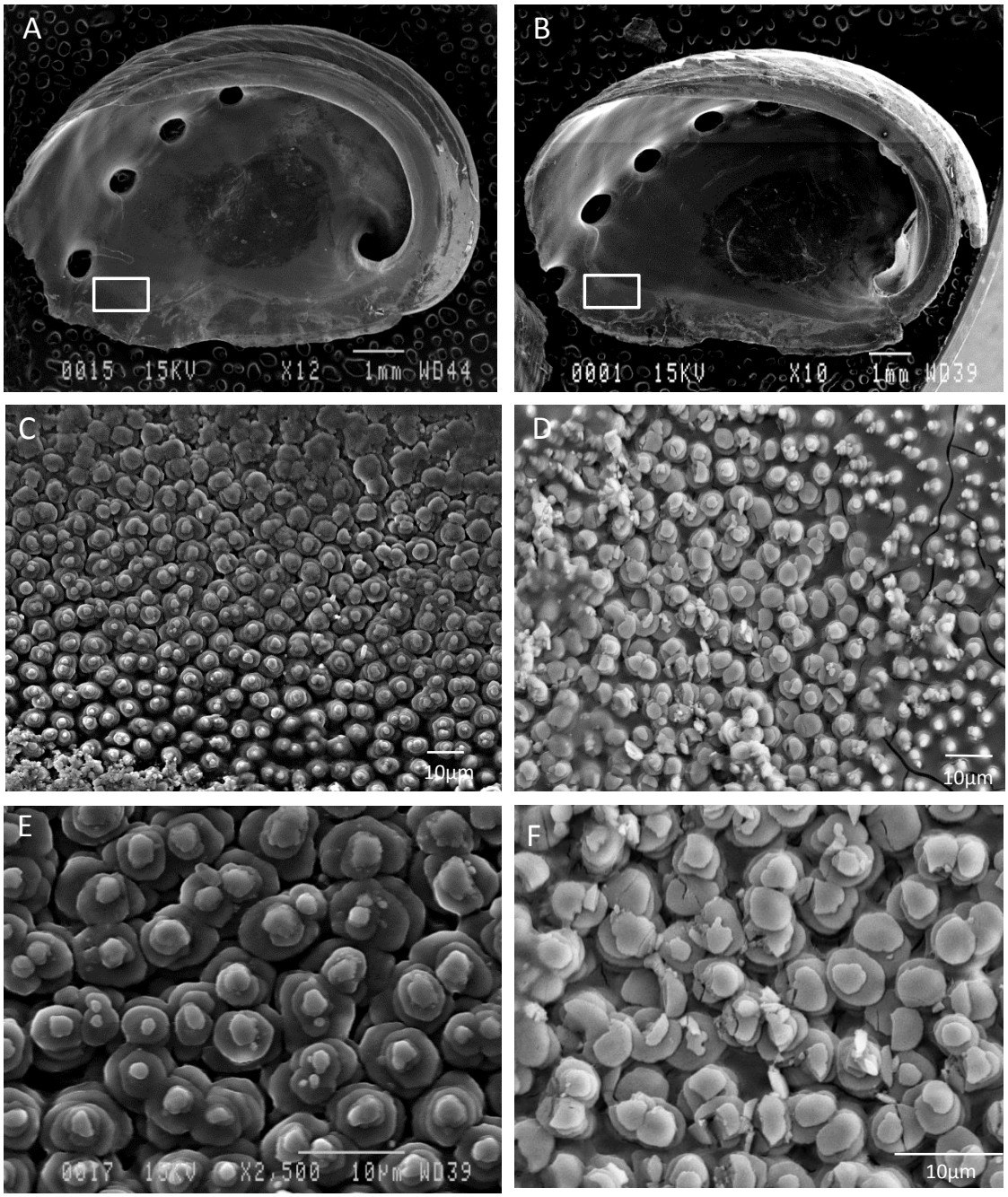


365

366 **Fig. 6** SEM images of abalone inner nacreous surface in control conditions ($pH_T$ 8.1: A, C, E)
367 and under low $pH_T$ 7.6 (B, D, F). **A.** Inner nacreous layer of control shell; **B.** Inner nacreous
368 layer of shell exposed to $pH_T$ 7.6; **C.** Detail of the nacre growth region boxed in A showing
369 gradual maturation of aragonite platelets; **D.** Detail of the nacre surface boxed in B showing
370 disruption of the aragonite platelets; **E.** Magnification of the nacre surface showing
371 confluence of regular aragonite platelets; **F.** Magnification of the nacre platelets showing
372 breaks within the platelets and irregularities of their edges.

373 Measurements along the shell section showed a progressive decrease of total shell thickness
374 from older to newly formed shell regions (results not shown), which is in accordance with the
375 shell growth process. Total shell thickness tended to be smaller in juveniles exposed to pH 7.6
376 compared with those reared under control $pH_T$ (unpaired t test, $t8 = -2.1644$, $P = 0.062$, Fig.
377 7a). However, a significant reduction of the spherulitic layer thickness was observed at $pH_T$
378 7.6 compared with the control group (unpaired t test, $t8 = -2.8522$, $P = 0.021$, Fig. 7b). There
379 was no significant differences in nacre shell thickness between abalones grown in these two
380 pH treatments (unpaired t test, $t8 = -0.4381$, $P = 0.67$).

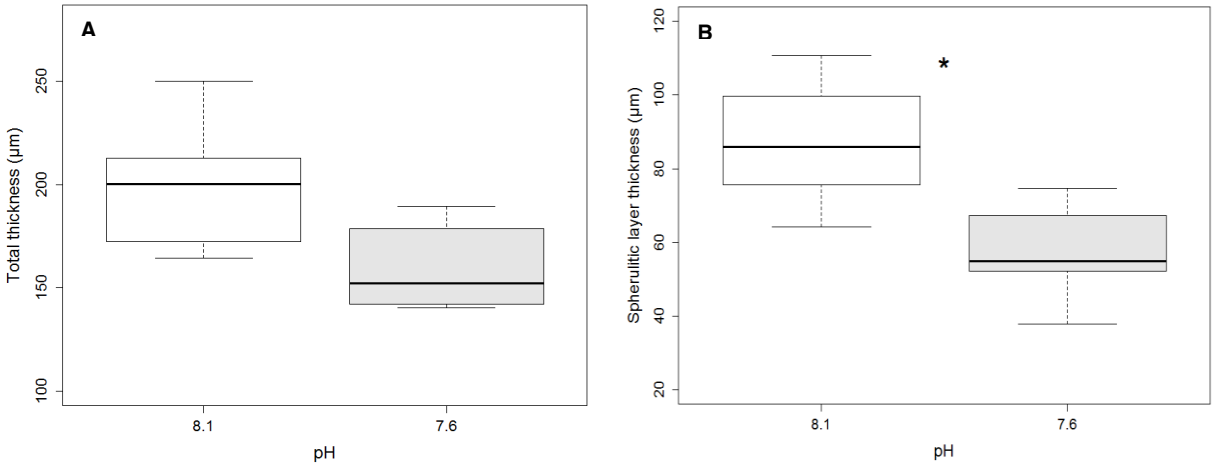


381

382 **Fig. 7** Total thickness (**A**) and spherulitic layer thickness (**B**) of juvenile abalone shells grown
383 under control $pH_T$ (8.1) and low $pH_T$ (7.6) treatment. Centre lines of box plots show the
384 medians; box limits indicate the first and third quartiles, respectively, with whiskers
385 encompassing data within 1.5 times the spread from the median (n = 5 per pH condition).
386 Asterisk indicates a significant difference between pH treatments (unpaired Student's t-test, $P$
387 $< 0.05$).

388 The shell fracture force was significantly lowered at $pH_T$ 7.6 compared with shells that had
389 grown in the three other pH treatments (ANOVA, $F(3,7) = 11.15$, $P = 0.0047$, Fig. 8, Table
390 3). However, because shell weight (and thickness) was reduced at low pH, the fracture force
391 was analysed according to weight. The regression of shell fracture force on abalone shell

weight showed a linear relationship (Linear regression, $r^2 = 0.63$, $F(1,41) = 68.42$, $P = 0.031$, Fig. 9). A test of homogeneity of slopes of the regression lines of shell fracture force vs weight showed that these were not significantly different between pH treatments (interaction pH * weight, $F(3,34) = 0.486$, $P = 0.69$, Table 4). Testing on the intercept with shell weight as a co-variable, showed that the effect of pH on shell fracture force was not significant (ANCOVA, $F(3,7) = 1.021$, $P = 0.44$). This indicates that the decreased fracture force at $pH_T$ 7.6 could be explained by the reduced amount of shell material only.

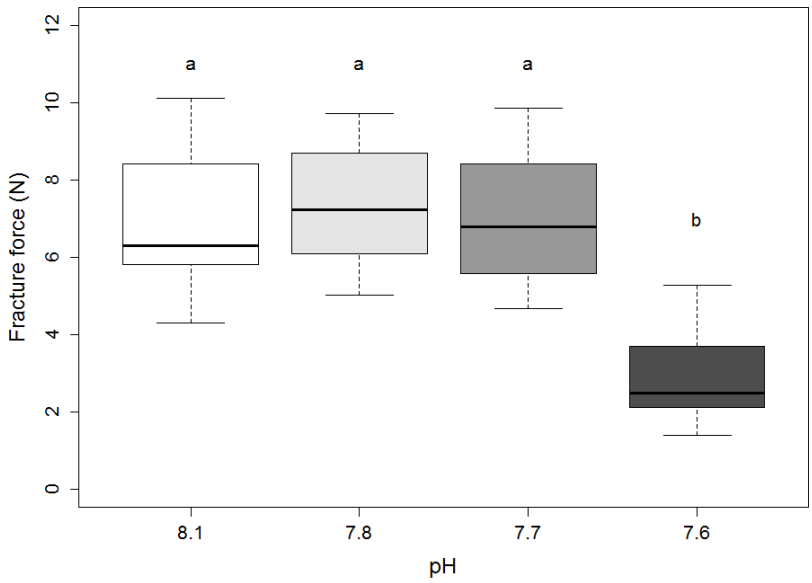


**Fig. 8** Fracture force of the shells of abalones reared under different pH conditions. Centre lines of box plots show the medians; box limits indicate the first and third quartiles, respectively, with whiskers encompassing data within 1.5 times the spread from the median (n = 12 for $pH_T$ 8.1 and 7.8; n = 11 for $pH_T$ 7.7; n = 7 for $pH_T$ 7.6). Different letters indicate significant differences between pH treatments ($P < 0.05$).

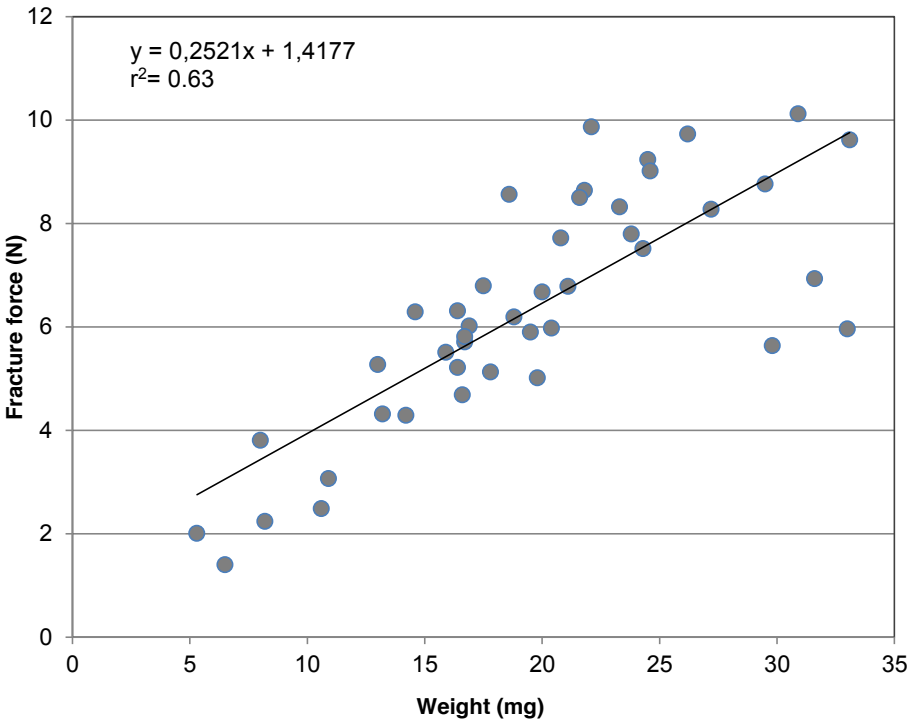


**Fig. 9** Linear regression of shell fracture force against abalone shell weight (n = 43) ($r^2$ = 0.63, $F(1,41)$ = 68.42, $P$ = 0.031).

## Discussion

The present study demonstrated that decreased pH negatively impacts the growth and shell mineralization of juvenile European abalone *Haliotis tuberculata*. Almost all the tested variables were significantly reduced at $pH_T$ 7.6 (0.5 units below control pH) while $pH_T$ 7.7 and 7.8 did not affect juvenile growth. These results are rather similar to those obtained in two other species of farmed abalone. In juvenile *H. iris*, Cunningham et al. (2016) reported significant effects on shell length and wet weight at $pH_{NBS}$ 7.6 in winter (corresponding to $pH_T$ 7.5) and at $pH_{NBS}$ 7.8 ($pH_T$ 7.7; 0.3 units below control pH) and 7.6 ($pH_T$ 7.5; 0.5 units below control pH) in summer. Similarly, shell growth and shell weight were significantly lower in juvenile *H. discus hannai* after 3 months of exposure to $pH_{NBS}$ 7.7 and 7.9 (corresponding respectively to $pH_T$ 7.8 and 7.6, Li et al. 2018). These results are also in

accordance with previous studies on other marine shelled mollusc taxa, showing significant reductions in shell growth following medium to long term exposure to near-future pH (reviewed in Gazeau et al. 2013). In a two-month experiment, Thomsen and Melzner (2010) observed significant decreases in both shell mass and shell length in blue mussels exposed to lowered pH (- 0.3 to - 0.9 units). Similarly, the mussel *Mytilus galloprovincialis* exhibited a slow-down of shell growth when pH was reduced by 0.75 units, possibly caused by dissolution (Michaelidis et al. 2005). As suggested in previous studies, the effects of OA on shell growth and calcification would result either from a direct effect on $CaCO_3$ dissolution or from indirect metabolic effects, such as physiological and molecular processes regulating shell biomineralization (Beniash et al. 2010; Hüning et al. 2012; Klok et al. 2014). The increasing cost of maintaining acid-base balance combined with an impaired ability to calcify under OA may explain the decrease in the scope for growth among early life stages of molluscs experiencing acidified conditions (Gazeau et al. 2013; Parker et al. 2013; Thomsen et al. 2015). However, Cunningham et al. (2016) found no changes in respiration rate of *H. iris* juveniles subjected to reduced pH (- 0.3 to - 0.5 units), indicating that abalone do not up-regulate their metabolism. Nothing is known on the acid-base balance regulation abilities of abalones but molluscs (apart from cephalopods) are usually considered to have a poor ability to compensate for decreasing haemolymph pH in situations of seawater acidification (Melzner et al. 2009). According to Cyronak et al. (2016), elevated $H^+$ concentration and subsequent problems of homeostasis rather than carbonate ions concentration, would be more likely responsible for the reduction of calcification in marine organisms facing OA.

Our results revealed significant changes in shell microstructure of juvenile abalones grown at $pH_T$ 7.6, including corrosion of the outer periostracum and degradation of the inner nacreous aragonite layer. In juvenile *H. discus hannai*, corroded periostracum was found in individuals grown at $pH_{NBS}$ 7.7 (Li et al. 2018), but the effect of decreased pH on shell microstructure was not investigated. Shell surface corrosion and changes in biomineral

464 microstructure under low pH have been previously reported in juvenile bivalves and related to
465 a direct effect on shell dissolution (Fitzer et al. 2014b; Hiebenthal et al. 2013; McClintock et
466 al. 2009; Melzner et al. 2011; Waldbusser et al. 2011). It is noteworthy that we only recorded
467 significant effects at $pH_T$ 7.6, the only treatment at which $\Omega_{aragonite}$ was lower than one. The
468 corrosion of the periostracum and degradation of the nacreous layer were observed both in the
469 old part and in the newly formed shell under the low pH, indicating that direct dissolution is
470 involved rather than indirect metabolic process affecting the synthesis of the new shell.
471 However, the energetic cost for proton elimination during $CaCO_3$ precipitation is increased
472 under elevated $pCO_2$, suggesting a metabolic effect.

473 This finding also supports the hypothesis that the effects on shell length and weight may be
474 mainly due to the shell dissolution. Indeed, the juvenile and adult shells of *H. tuberculata*
475 consist of two biomineralized layers, the outer spherulitic and the inner nacreous layers, both
476 composed of the aragonite $CaCO_3$ polymorph (Auzoux-Bordenave et al. 2010, 2015; Jardillier
477 et al. 2008). The predominance of aragonite in the *H. tuberculata* shell makes the species
478 more susceptible to dissolution than other mollusc species with calcitic shells or a
479 calcite/aragonite mixture (Gazeau et al. 2013; Parker et al. 2013). In the course of a trans-
480 generational experiment on juvenile *M. edulis* exposed to elevated $pCO_2$, Fitzer et al. (2014a)
481 revealed that mussels at high $pCO_2$ (1000µatm) did not produce aragonite, which is more
482 vulnerable to carbonate under-saturation than calcite. Under lower $pCO_2$ (550, 750 µatm), the
483 nacreous tablets formed the usual 'brick wall' structure, although the nacre crystals appeared
484 corroded and were not so closely stacked together as under normal conditions (Fitzer et al.
485 2014a). This could indicate reduced biological control over biomineralization of aragonite by
486 the organism and potentially raises questions about the integrity of mollusc shells composed
487 only of aragonite under OA.

488 In addition to changes in shell microstructure, we found a significant reduction in the
489 spherulitic shell thickness and, to a lesser extent, in the total thickness of abalone shells grown

490 at $pH_T$ 7.6. The reduction of shell thickness is likely due to $CaCO_3$ dissolution of the outer
491 aragonite layer, which would be more sensitive to OA after periostracum corrosion. In
492 juvenile shells of *M. edulis*, a reduction in shell thickness was reported in the aragonite layer,
493 but not in the calcite layer, after 6 months of exposure to elevated $pCO_2$ (Fitzer et al. 2014b).
494 Other juvenile bivalves (*Argopecten irradians* and *Mercenaria mercenaria*) grown under
495 increased $CO_2$ concentration (corresponding to a reduction of 0.4 to 0.6 pH units), also
496 exhibited malformed and corroded shells with reduced thickness (Talmage and Gobler 2010).
497 Welladsen et al. (2010) also reported a significant decrease in shell strength and nacre
498 malformation in the adult pearl oyster *Pinctada fucata* exposed to acidified seawater ($pH_{NBS}$
499 7.6), suggesting shell dissolution.

500 The integrity of the periostracum (the organic coating of the mollusc shell) is very
501 important for protecting the shell from corrosion induced by low pH (Thomsen et al. 2010). In
502 juvenile abalone, we found that the periostracum was damaged under low pH, resulting in a
503 higher vulnerability of the underlying mineralized layers. Indeed, a subsequent reduction in
504 thickness of the spherulitic layer as well as changes in the nacreous layer microstructure were
505 observed. These observations are consistent with those reported for other shellfish reared
506 under lowered pH (Talmage and Gobler 2010). All of this suggests that processes leading to
507 the synthesis of the periostracum are affected by low pH, implying that the kinetics of
508 aragonite precipitation (evidenced by the reduced growth rate) and the thermodynamics of its
509 dissolution (due to under saturated sea water in the $pH_T$ 7.6 treatment) are not the only aspects
510 of the shell being affected. Potential effects of decreased pH on shell organic components
511 (chitin and matrix proteins) may explain the corrosion of the periostracum and some of the
512 changes observed in the nacre microstructure, but the underlying mechanisms are far from
513 being understood (Fitzer et al. 2014b; Hüning et al. 2012). A number of indirect biological
514 processes involved in shell calcification, such as matrix protein production, chitin synthesis
515 and enzymatic control are influenced by changes in seawater $pCO_2$ (Weiss et al. 2013). In the

516 mussel *M. edulis*, six months of incubation at 750 µatm $pCO_2$ ($pH_T$ 7.5) significantly reduced
517 carbonic anhydrase activity within the mantle tissue, explaining shell growth reduction (Fitzer
518 et al. 2014b). In another study of *M. edulis*, a strong depression in the expression of mRNA
519 for a chitinase, an enzyme involved in the calcification process, was correlated with a linear
520 decrease in shell growth (Hüning et al. 2012). Interestingly, this study also found that
521 expression of several genes, including some genes involved in shell protection and/or
522 periostracum formation (tyrosinase) increased in response to elevated $pCO_2$ (Hüning et al.
523 2012). By contrast, despite evidence of shell dissolution, no difference was found in the
524 organic content or periostracum integrity of adult *P. fucata* shells exposed to $pH_{NBS}$ 7.6
525 (Welladsen et al. 2010). However, the authors noted that because the study was conducted
526 over only a 28-day period, it did not allow acclimation of the oysters to the acidified
527 conditions.

528 In juvenile *H. tuberculata*, the significant reduction in shell fracture force at $pH_T$ 7.6 can be
529 explained by the reduced shell weight. This probably results from both reduced growth and
530 shell dissolution. A smaller (isometric) dome is submitted to a higher meridional compressive
531 stress for the same external force applied and will therefore rupture at a lower applied force
532 (Vogel 2003). Shell dissolution will induce an easier induction of cracks and cleavage, probably
533 initiated by dissolution pits inducing stress concentration at their level (Mc Neill 1968). Both
534 effects would increase the period during which abalone are exposed to strong predation pressure
535 before they reach a refuge in size and shell strength. This would have an economic impact on
536 abalone aquaculture as it would increase the time required to reach a marketable size and
537 possibly enhance productivity losses through shell breakage during handling.

538 Marine molluscs exert a strong control on the calcification process, but their capacities to
539 maintain optimal conditions at the site of calcification when facing OA stress remain largely
540 unknown (Gazeau et al. 2013; Parker et al. 2013). Because shell calcification has a high
541 energetic cost and is very sensitive to OA (especially in early stages), energy usually allocated

542 to growth and reproduction might be partially reallocated to calcification (Thomsen and
543 Melzner 2010). The capacity of abalone to grow in the near future will depend on their
544 potential to maintain their vital functions (reproduction, growth and biomineralization) under
545 modified environmental conditions. Since responses to OA may also differ according to
546 differences in physiology, habitat and behaviour of the species (Gazeau et al. 2013), the local
547 seasonal variations in physico-chemical conditions should be considered in further studies on
548 adaptive responses. The seawater $pH_T$ along the Brittany coast in France naturally varies from
549 7.9 to 8.2 (Qui-Minet et al. 2018), so that a future scenario testing a decrease of - 0.3 units
550 from ambient $pH_T$ is consistent with seasonal or diurnal variations presently experienced by
551 abalone in the tidal zone. Indeed, seasonal variations in pH are close to 0.3 units in shallow
552 subtidal environments (Qui-Minet et al. 2018), while diurnal variations of $pH_T$ in the intertidal
553 zone can be higher. For instance, pH can fall down to $pH_T$ 7.5 in rock pools along the Brittany
554 coast during night-time emersion at low tide (Legrand et al. 2018). Thus, abalone from
555 Brittany shoreline environments might already experience chronically pH similar to global
556 average pH levels predicted for open ocean by 2100 (ie. $pH_T$ 7.7). Such fluctuations of pH in
557 their coastal habitats might explain the potential resistance of abalone to $pH_T > 7.6$.

558 The results of our study indicate that a decrease of 0.5 pH units significantly reduces
559 growth, shell calcification and shell strength of juvenile abalone *H. tuberculata*. In the natural
560 environment, where juvenile stages are exposed to a strong predation pressure, abalone may
561 be at greater risk under future pH conditions as their shells may not offer sufficient protection
562 from predators and other external stressors. Understanding how different abalone life stages
563 respond to OA will make it possible to identify bottlenecks for population persistence under
564 near-future pH conditions. These findings also highlight the importance of monitoring
565 seawater parameters in aquaculture systems, where effort can be directed to maintaining
566 seawater pH at key periods of abalone culture to minimize stress and prevent production
567 losses.

## Acknowledgements

N. Wessel was supported by a postdoctoral fellowship from the MNHN (*Ministère de l'Enseignement Supérieur et de la Recherche*, Paris, France). This work was supported in part by the ATM program "Biomineralization" of the MNHN funded by the *Ministère délégué à l'Enseignement Supérieur et à la Recherche* (Paris, France) and by the ICOBio project under the program "*Acidification des Océans*" funded by the Fondation pour la Recherche sur la Biodiversité (FRB) and the *Ministère de la Transition Ecologique et Solidaire* (MTES). We thank Dr. Chakib Djejat and Stéphane Formosa for their assistance in scanning electron microscopy (SEM, *Plateau technique de Microscopie Electronique*, MNHN, Paris and Concarneau, France). The Regional Council of Brittany, the General Council of Finistère, the urban community of *Concarneau Cornouaille Agglomération* and the European Regional Development Fund (ERDF) are acknowledged for the funding of the Sigma 300 FE-SEM of the Concarneau Marine Station. We thank Dr. Cedric Hubas for his valuable support for the statistical analyses and the Translation Bureau of the University of Western Brittany for improving the English of this manuscript. We also thank the 3 anonymous reviewers for their comments which have helped to improve this manuscript. Ph. Dubois is a Research Director of the National Fund for Scientific Research (Belgium).

## Compliance with ethical standards

The authors declare that they have no conflicts of interest or competing financial interests.

The experiments complied with the current French laws. All applicable international, national, and institutional guidelines for the care and use of animals were followed.

592 **References**

593


594 Auzoux-Bordenave S, Badou A, Gaume B, Berland S, Helléouet M-N, Milet C, Huchette S
595 (2010) Ultrastructure, chemistry and mineralogy of the growing shell of the European
596 abalone *Haliotis tuberculata*. J Struct Biol 171:277–290. doi: 10.1016/j.jsb.2010.05.012

597 Auzoux-Bordenave S, Brahmi C, Badou A, De Rafélis M, Huchette S (2015) Shell growth,
598 microstructure and composition over the development cycle of the European abalone
599 *Haliotis tuberculata*. Mar Biol 162:687–697. doi: 10.1007/s00227-015-2615-y

600 Beniash E, Ivanina A, Lieb NS, Kurochkin I, Sokolova IM (2010) Elevated level of carbon
601 dioxide affects metabolism and shell formation in oysters *Crassostrea virginica*. Mar
602 Ecol Prog Ser 419:95–108. doi: 10.3354/meps08841

603 Byrne M, Ho M, Wong E, Soars NA, Selvakumaraswamy P, Shepard-Brennand H,
604 Dworjanyn SA, Davis AR (2011) Unshelled abalone and corrupted urchins:
605 development of marine calcifiers in a changing ocean. Proc R Soc B Biol Sci 278:2376–
606 2383. doi: 10.1098/rspb.2010.2404

607 Cook PA (2014) The worldwide abalone industry. Mod Econ 05:1181–1186. doi:
608 10.4236/me.2014.513110

609 Courtois de Viçose G, Viera MP, Bilbao A, Izquierdo MS (2007) Embryonic and larval
610 development of *Haliotis tuberculata coccinea* Reeve: an indexed micro-photographic
611 sequence. J Shellfish Res 26:847–854. doi: 10.2983/0730-
612 8000(2007)26[847:EALDOH]2.0.CO;2

613 Crim RN, Sunday JM, Harley CDG (2011) Elevated seawater $CO_2$ concentrations impair
614 larval development and reduce larval survival in endangered northern abalone (*Haliotis*
615 *kamtschatkana*). J Exp Mar Biol Ecol 400:272–277. doi: 10.1016/j.jembe.2011.02.002

616 Cunningham SC, Smith AM, Lamare MD (2016) The effects of elevated $pCO_2$ on growth,
617 shell production and metabolism of cultured juvenile abalone, *Haliotis iris*. Aquac Res
618 47:2375–2392. doi: 10.1111/are.12684

619 Cyronak T, Schulz KG, Jokiel PL (2016) The Omega myth: what really drives lower
620 calcification rates in an acidifying ocean. ICES J Mar Sci 73: 558–562
621 doi:10.1093/icesjms/fsv075

622 Day RW, Quinn GP (1989) Comparisons of treatments after an analysis of variance in
623 ecology. Ecol Monogr 59:433–463. doi: 10.2307/1943075

624 Dickson AG (2010) Standards for ocean measurements. Oceanography 23:34–47. doi:
625 10.5670/oceanog.2010.22

626 Dickson AG, Millero FJ (1987) A comparison of the equilibrium constants for the
627 dissociation of carbonic acid in seawater media. Deep-Sea Res 34:1733–1743.

628 Dickson AG, Sabine CL, Christian JR (2007) Guide to best practices for ocean $CO_2$
629 measurements. PICES Spec Publ 3:191.

630 Doney SC, Fabry VJ, Feely RA, Kleypas JA (2009) Ocean acidification: the other $CO_2$
631 problem. Annu Rev Mar Sci 1:169–192. doi: 10.1146/annurev.marine.010908.163834

632 Duquette A, McClintock JB, Amsler CD, Pérez-Huerta A, Milazzo M, Hall-Spencer JM,
633 (2017) Effects of ocean acidification on the shells of four Mediterranean gastropod
634 species near a $CO_2$ seep. Mar Pollut Bull 124 : 917-928.
635 https://doi.org/10.1016/j.marpolbul.2017.08.007

636 Ekstrom JA, Suatoni L, Cooley SR, Pendleton LH, Waldbusser GG, Cinner JE, Ritter J,
637 Langdon C, Van Hooidonk R, Gledhill D, Wellman K, Beck MW, Brander LM,
638 Rittschof D, Doherty C, Edwards PET, Portela R (2015) Vulnerability and adaptation of

639 US shellfisheries to ocean acidification. Nat Clim Change 5:207–214. doi:
640 10.1038/nclimate2508

641 Ellis RP, Bersey J, Rundle SD, Hall-Spencer JM, Spicer JI (2009) Subtle but significant
642 effects of $CO_2$ acidified seawater on embryos of the intertidal snail, *Littorina obtusata*.
643 Aquat Biol 5:41–48. doi: 10.3354/ab00118

644 Fitzer SC, Cusack M, Phoenix VR, Kamenos NA (2014a) Ocean acidification reduces the
645 crystallographic control in juvenile mussel shells. J Struct Biol 188:39–45. doi:
646 10.1016/j.jsb.2014.08.007

647 Fitzer SC, Phoenix VR, Cusack M, Kamenos NA (2014b) Ocean acidification impacts mussel
648 control on biomineralisation. Sci Rep 4:6218. doi: 10.1038/srep06218

649 Gallardo WG, Bautista-Teruel MN, Fermin AC, Marte CL (2003) Shell marking by artificial
650 feeding of the tropical abalone *Haliotis asinina* Linne juveniles for sea ranching and
651 stock enhancement. Aquac. Res. 34, 839-842).

652 Gattuso JP, Magnan A, Bille R, Cheung WWL, Howes EL, Joos F, Allemand D, Bopp L,
653 Cooley SR, Eakin CM, Hoegh-Guldberg O, Kelly RP, Portner HO, Rogers AD, Baxter
654 JM, Laffoley D, Osborn D, Rankovic A, Rochette J, Sumaila UR, Treyer S, Turley C
655 (2015) Contrasting futures for ocean and society from different anthropogenic $CO_2$
656 emissions scenarios. Science 349:4722–4722. doi: 10.1126/science.aac4722

657 Gazeau F, Quiblier C, Jansen JM, Gattuso J-P, Middelburg JJ, Heip CHR (2007) Impact of
658 elevated $CO_2$ on shellfish calcification. Geophys Res Lett. doi: 10.1029/2006gl028554

659 Gazeau F, Gattuso JP, Dawber C, Pronker AE, Peene F, Peene J, Heip CHR, Middelburg JJ
660 (2010) Effect of ocean acidification on the early life stages of the blue mussel *Mytilus*
661 *edulis*. Biogeosciences 7:2051–2060. doi: 10.5194/bg-7-2051-2010

662 Gazeau F, Parker LM, Comeau S, Gattuso J-P, O'Connor WA, Martin S, Pörtner H-O, Ross
663 PM (2013) Impacts of ocean acidification on marine shelled molluscs. Mar Biol
664 160:2207–2245. doi: 10.1007/s00227-013-2219-3

665 Guo X, Huang M, Pu F, You W, Ke C (2015) Effects of ocean acidification caused by rising
666 $CO_2$ on the early development of three mollusks. Aquat Biol 23:147–157. doi:
667 10.3354/ab00615

668 Hendriks IE, Duarte CM, Álvarez M (2010) Vulnerability of marine biodiversity to ocean
669 acidification: A meta-analysis. Estuar Coast Shelf Sci 86:157–164. doi:
670 10.1016/j.ecss.2009.11.022

671 Hiebenthal C, Philipp EER, Eisenhauer A, Wahl M (2013) Effects of seawater $pCO_2$ and
672 temperature on shell growth, shell stability, condition and cellular stress of Western
673 Baltic Sea *Mytilus edulis* (L.) and *Arctica islandica* (L.). Mar Biol 160: 2073–2087. doi:
674 10.1007/s00227-012-2080-9

675 Hofmann GE, Barry JP, Edmunds PJ, Gates RD, Hutchins DA, Klinger T, Sewell MA (2010)
676 The effect of ocean acidification on calcifying organisms in marine ecosystems: an
677 organism to-ecosystem perspectiv. Annu Rev Ecol Evol Syst 41:127–147. doi:
678 10.1146/annurev.ecolsys.ll0308.120227

679 Huchette S, Clavier J (2004) Status of the ormer (*Haliotis tuberculata* L.) industry in Europe.
680 J Shellfish Res 23:951–955.

681 Hüning AK, Melzner F, Thomsen J, Gutowska MA, Krämer L, Frickenhaus S, Rosenstiel P,
682 Pörtner H-O, Philipp EER, Lucassen M (2012) Impacts of seawater acidification on
683 mantle gene expression patterns of the Baltic Sea blue mussel: implications for shell
684 formation and energy metabolism. Mar Biol. doi: 10.1007/s00227-012-1930-9

685 IPCC (2014) Summary for Policymakers. In: Climate Change 2014: Impacts, Adaptation, and
686 Vulnerability. Part A: Global and Sectoral Aspects. Contribution of Working Group II
687 to the Fifth Assessment Report of the Intergovernmental Panel on Climate Change.
688 Cambridge University Press, Cambridge, United Kingdom and New York, NY, USA,
689 pp 1–32

690 Jardillier E, Rousseau M, Gendron-Badou A, Fröhlich F, Smith DC, Martin M, Helléouet M-
691 N, Huchette S, Doumenc D, Auzoux-Bordenave S (2008) A morphological and
692 structural study of the larval shell from the abalone Haliotis tuberculata. Mar Biol, 154
693 (4): 735-744,

694 Kimura RYO, Takami H, Ono T, Onitsuka T, Nojiri Y (2011) Effects of elevated $pCO_2$ on the
695 early development of the commercially important gastropod, Ezo abalone *Haliotis*
696 *discus hannai*. Fish Oceanogr 20:357–366. doi: 10.1111/j.1365-2419.2011.00589.x

697 Klok C, Wijsman JWM, Kaag K, Foekema E (2014) Effects of $CO_2$ enrichment on cockle
698 shell growth interpreted with a Dynamic Energy Budget model J Sea Res 94 : 111–116

699 Kroeker KJ, Kordas RL, Crim RN, Singh GG (2010) Meta-analysis reveals negative yet
700 variable effects of ocean acidification on marine organisms. Ecol Lett 13:1419–1434.
701 doi: 10.1111/j.1461-0248.2010.01518.x

702 Kurihara H (2008) Effects of $CO_2$-driven ocean acidification on the early developmental
703 stages of invertebrates. Mar Ecol Prog Ser 373:275–284. doi: 10.3354/meps07802

704 Legrand E, Riera P, Pouliquen L, Bohner O, Cariou T, Martin S (2018) Ecological
705 characterization of intertidal rockpools: Seasonal and diurnal monitoring of physico-
706 chemical parameters. Reg Stud Mar Sci 17:1–10. doi: 10.1016/j.rsma.2017.11.003

Li J, Mao Y, Jiang Z, Zhang J, Fang J, Bian D (2018) The detrimental effects of $CO_2$-driven chronic acidification on juvenile Pacific abalone (*Haliotis discus hannai*). Hydrobiologia 809, 297-308. https://doi.org/10.1007/s10750-017-3481-z

Marchais, V., Jolivet, A., Herve, S., Roussel, S., Schone, B.R., Grall, J., Chauvaud, L., Clavier, J., 2017. New tool to elucidate the diet of the ormer *Haliotis tuberculata* (L.): Digital shell color analysis. Mar. Biol. 164 (4): 1-13.

Martin S, Richier S, Pedrotti ML, Dupont S, Castejon C, Gerakis Y, Kerros ME, Oberhansli F, Teyssie JL, Jeffree R, Gattuso JP (2011) Early development and molecular plasticity in the Mediterranean sea urchin *Paracentrotus lividus* exposed to $CO_2$-driven acidification. J Exp Biol 214:1357–1368. doi: 10.1242/jeb.051169

McClintock JB, Angus RA, Mcdonald MR, Amsler CD, Catledge SA, Vohra YK (2009) Rapid dissolution of shells of weakly calcified Antarctic benthic macroorganisms indicates high vulnerability to ocean acidification. Antarct Sci 21:449–456. doi: 10.1017/S0954102009990198

McNeill, A. R. 1968. Animal Mechanics; Sidgwick and Jackson, London, United Kingdom.

Mehrbach C, Culberson CH, Hawley JE, Pytkowicx RM (1973) Measurement of the apparent dissociation constants of carbonic acid in seawater at atmospheric pressure. Limnol Oceanogr 18:897–907. doi: 10.4319/lo.1973.18.6.0897

Melzner F, Gutowska MA, Langenbuch M, Dupont S, Lucassen M, Thorndyke MC, Bleich M, Portner HO (2009) Physiological basis for high $CO_2$ tolerance in marine ectothermic animals: pre-adaptation through lifestyle and ontogeny? Biogeosciences 6:2313–2331.

Melzner F, Stange P, Trübenbach K, Thomsen J, Casties I, Panknin U, Gorb SN, Gutowska MA (2011) Food supply and seawater $pCO_2$ impact calcification and internal shell

730 dissolution in the blue mussel *Mytilus edulis*. PLOS ONE. doi:
731 10.1371/journal.pone.0024223.

732 Mercer JP, Mai KS, Donlon J (1993) Comparative studies on the nutrition of 2 species of
733 abalone, *Haliotis tuberculata Linnaeus* and *Haliotis discus hannai Ino* . 1. Effects of
734 algal diets on growth and biochemical composition. Invertebr Reprod Dev 23: 75-88.

735 Michaelidis B, Ouzounis C, Paleras A, Pörtner H-O (2005) Effects of long-term moderate
736 hypercapnia on acid–base balance and growth rate in marine mussels *Mytilus*
737 *galloprovincialis*. Mar Ecol Prog Ser 293:109–118.

738 Morash AJ, Alter K (2015) Effects of environmental and farm stress on abalone physiology:
739 perspectives for abalone aquaculture in the face of global climate change. Rev Aquac
740 7:1–27. doi: 10.1111/raq.12097

741 Morse JW, Arvidson RS, Luttge A (2007) Calcium carbonate formation and dissolution :
742 Chemical Reviews, 107: 342–381, doi: 10.1021/cr050358j.

743 Nicolas JL, Basuyaux O, Mazurié J, Thébault A (2002) *Vibrio carchariae*, a pathogen of the
744 abalone *Haliotis tuberculata*. Dis Aquat Organ 50:35–43.

745 Noisette F, Comtet T, Legrand E, Bordeyne F, Davoult D, Martin S (2014) Does
746 encapsulation protect embryos from the effects of ocean acidification? The example of
747 *Crepidula fornicata*. PLOS ONE. doi: 10.1371/journal.pone.0093021

748 Onitsuka T, Takami H, Muraoka D, Matsumoto Y, Nakatsubo A, Kimura R, Ono T, Nojiri Y
749 (2018). Effects of ocean acidification with $pCO_2$ diurnal fluctuations on survival and
750 larval shell formation of Ezo abalone, *Haliotis discus hannai*. Mar . Environ. Res. 134,
751 28-36. https://doi.org/10.1016/j.marenvres.2017.12.015²

752 Orr JC, Fabry VJ, Aumont O, Bopp L, Doney SC, Feely RA, Gnanadesikan A, Gruber N,
753 Ishida A, Joos F, Key RM, Lindsay K, Maier-Reimer E, Matear R, Monfray P, Mouchet
754 A, Najjar RG, Plattner G-K, Rodgers KB, Sabine CL, Sarmiento JL, Schlitzer R, Slater
755 RD, Totterdell IJ, Weirig M-F, Yamanaka Y, Yool A (2005) Anthropogenic ocean
756 acidification over the twenty-first century and its impact on calcifying organisms.
757 Nature 437:681–686. doi: 10.1038/nature04095

758 Parker L, Ross P, O'Connor W, Pörtner H, Scanes E, Wright J (2013) Predicting the response
759 of molluscs to the impact of ocean acidification. Biology 2:651–692. doi:
760 10.3390/biology2020651

761 Pierrot DE, Lewis E, Wallace D W R (2006) MS Excel program developed for CO2 system
762 calculations. ORNL/CDIAC-105a. Carbon Dioxide Information Analysis Center. Oak
763 Ridge National Laroratory, US Department of Energy, Oak Ridge, Tennessee.

764 Przeslawski R, Byrne M, Mellin C (2015) A review and meta-analysis of the effects of
765 multiple abiotic stressors on marine embryos and larvae. Glob Change Biol 21:2122–
766 2140. doi: 10.1111/gcb.12833

767 Qui-Minet ZN, Delaunay C, Grall J, Six C, Cariou T, Bohner O, Legrand E, Davoult D,
768 Martin S (2018) The role of local environmental changes on maerl and its associated
769 non-calcareous epiphytic flora in the Bay of Brest. Estuar Coast Shelf Sci 208:140–152.
770 doi: 10.1016/j.ecss.2018.04.032

771 R Core Team (2015) R Core Team: A language and environment for statistical computing.
772 Vienna, Austria

773 Riebesell U, Fabry VJ, Hansson L, Gattuso JP (2010) Guide to best practices for ocean
774 acidification research and data reporting, Publications Office of the European Union.

775 Ross PM, Parker L, O'Connor WA, Bailey EA (2011) The impact of ocean acidification on
776 reproduction, early development and settlement of marine organisms. Water 3:1005–
777 1030. doi: 10.3390/w3041005

778 Shepherd SA (1973) Studies on southern Australian abalone (genus *Haliotis*). I. Ecology of
779 five sympatric species. Aust. J. Mar. Freshwat. Res. 24, 217-257.

780 Talmage SC, Gobler CJ (2010) Effects of past, present, and future ocean carbon dioxide
781 concentrations on the growth and survival of larval shellfish. PNAS 107:17246–17251.
782 doi: 10.1073/pnas.0913804107

783 Thomsen J, Gutowska MA, Saphörster J, Heinemann A, Trübenbach K, Fietzke K,
784 Hiebenthal C, Eisenhauer A, Körtzinger A, Wahl M, Melzner F (2010) Calcifying
785 invertebrates succeed in a naturally CO2-rich coastal habitat but are threatened by high
786 levels of future acidification. Biogeosciences 7:3879–3891. doi.org/10.5194/bg-7-3879-
787 2010

788 Thomsen J, Melzner F (2010) Moderate seawater acidification does not elicit long-term
789 metabolic depression in the blue mussel *Mytilus edulis*. Mar Biol 157:2667–2676. doi:
790 10.1007/s00227-010-1527-0

791 Thomsen J, Haynert K, Wegner KM, Melzner F (2015) Impact of seawater carbonate
792 chemistry on the calcification of marine bivalves. Biogeosciences 12:4209–4220. doi:
793 10.5194/bg-12-4209-2015

794 Travers M-A, Basuyaux O, Le Goic N, Huchette S, Nicolas J-L, Koken M, Paillard C (2009)
795 Influence of temperature and spawning effort on *Haliotis tuberculata* mortalities caused
796 by *Vibrio harveyi*: an example of emerging vibriosis linked to global warming. Glob
797 Change Biol 15:1365–1376. doi: 10.1111/j.1365-2486.2008.01764.x

798 Vogel S. 2003. Comparative Biomechanics. Princeton University Press, Princeton, USA.

799 Waldbusser GG, Steenson RA, Green MA (2011) Oyster shell dissolution rates in estuarine
800 waters: effects of pH and shell legacy. J Shellfish Res 30:659–670.

801 Weiss IM, Lüke F, Eichner N, Guth C, Clausen-Schaumann H (2013) On the function of
802 chitin synthase extracellular domains in biomineralization. J Struct Biol 183:216–225.
803 doi: 10.1016/j.jsb.2013.04.011

804 Welladsen HM, Southgate PC, Heimann K (2010) The effects of exposure to near-future
805 levels of ocean acidification on shell characteristics of *Pinctada fucata* (Bivalvia:
806 Pteriidae). Molluscan Res 30:125–130.

807 Wessel N, Martin S, Badou A, Dubois P, Huchette S, Julia V, Nunes F, Harney E, Paillard C,
808 Auzoux-Bordenave S (2018) Effect of $CO_2$–induced ocean acidification on the early
809 development and shell mineralization of the European abalone *Haliotis tuberculata*. J
810 Exp Mar Biol Ecol 508:52–63.

811 Widdicombe S, Spicer JI (2008) Predicting the impact of ocean acidification on benthic
812 biodiversity: What can animal physiology tell us? J Exp Mar Biol Ecol 366:187–197.
813 doi: 10.1016/j.jembe.2008.07.024

814 Wittmann AC, Pörtner H-O (2013) Sensitivities of extant animal taxa to ocean acidification.
815 Nat Clim Change 3: 995-1001. doi: 10.1038/NCLIMATE1982

816 Zippay ML, Hofmann GE (2010) Effect of pH on gene expression and thermal tolerance of
817 early life history stages of red abalone (*Haliotis rufescens*). J Shellfish Res 29:429–439.

818

Table 1

**Table 1** Parameters of seawater carbonate chemistry during the experiment (means ± SD). pH on the total scale ($pH_T$), temperature (°C), salinity and total alkalinity ($\mu Eq.kg^{-1}$) were used to calculate $CO_2$ partial pressure ($pCO_2$; µatm), Dissolved Inorganic Carbon (DIC; µmol. $kg^{-1}$), $HCO_3^-$, $CO_3^{2-}$, aragonite saturation state ($\Omega_{aragonite}$) and calcite saturation state ($\Omega_{calcite}$) by using the CO2SYS program. $pH_T$ and temperature are the average values recorded almost daily throughout the experiment (n = 76 per pH treatment). Salinity was measured twice a week (mean 35.3 ± 1.3, n = 26) and total alkalinity was measured every two weeks throughout the experiment (n = 8 per pH treatment).

| Nominal pH | $pH_T$ | Temperature (°C) | TA (µEq/kg) | $pCO_2$ (µatm) | DIC (µmol.$kg^{-1}$) | $HCO_3^-$ (µmol.$kg^{-1}$) | $CO_3^{2-}$ (µmol.$kg^{-1}$) | $\Omega_{aragonite}$ | $\Omega_{calcite}$ |
|---|---|---|---|---|---|---|---|---|---|
| 8.1 | 8.11 ± 0.04 | 12.4 ± 1.8 | 2305 ± 28 | 335 ± 33 | 2070 ± 22 | 1890 ± 35 | 167 ± 14 | 2.53 ± 0.22 | 3.96 ± 0.34 |
| 7.8 | 7.81 ± 0.05 | 12.1 ± 1.7 | 2312 ± 30 | 750 ± 18 | 2209 ± 18 | 2088 ± 24 | 90 ± 10 | 1.37 ± 0.15 | 2.14 ± 0.23 |
| 7.7 | 7.71 ± 0.04 | 12.3 ± 1.7 | 2308 ± 37 | 958 ± 108 | 2237 ± 17 | 2124 ± 20 | 74 ± 8 | 1.12 ± 0.13 | 1.75 ± 0.2 |
| 7.6 | 7.60 ± 0.05 | 12.1 ± 1.8 | 2309 ± 34 | 1259 ± 140 | 2274 ± 16 | 2164 ± 17 | 58 ± 7 | 0.88 ± 0.1 | 1.38 ± 0.16 |

**Table 2** Summary of statistics **A.** Nested ANOVA results of the effects of pH on shell length, weight, relative growth and Welch test on shell density index in juvenile abalone *H. tuberculata* (pH: fixed factor, tank: random factor nested into pH). **B.** Multiple comparison Tukey's HSD Test testing the influence of pH on shell length and weight and Welch test on shell density index in juvenile abalone *H. tuberculata*. Significant *P*-values in bold ($P < 0.05$).

**A.**

| **Shell length** | SS | df | MS | *F*-ratio | *P*-value |
|---|---|---|---|---|---|
| pH | 14.66 | 3 | 4.89 | 4.78 | **0.034** |
| Residuals | 8.18 | 8 | 1.02 | | |
| Error (tank) | 131.6 | 129 | 1.02 | | |
| **Shell weight** $^{\alpha}$ | | | | | |
| pH | 1.28 | 3 | 0.42 | 24.43 | **<0.001** |
| Residuals | 0.14 | 8 | 0.02 | | |
| Error (tank) | 1.41 | 67 | 0.02 | | |
| **Relative shell growth** | | | | | |
| pH | 0.034 | 3 | 0.11 | 0.626 | 0.618 |
| Residuals | 0.147 | 8 | 0.02 | | |
| Error (tank) | 0.752 | 126 | 0.006 | | |
| **Shell density index** $^{\delta}$ | | | | | |
| pH | - | 3 | - | 14.47 | **0.013** |

$^{\alpha}$ Log transformation ; $^{\delta}$ Welch test

**B.**

| pH groups | 7.6/7.7 | 7.6/7.8 | 7.6/8.1 | 7.7/7.8 | 7.7/8.1 | 7.8/8.1 |
|---|---|---|---|---|---|---|
| Shell length | 0.736 | **0.027** | 0.305 | 0.119 | 0.838 | 0.347 |
| Shell weight | **< 0.005** | **< 0.001** | **< 0.001** | 0.139 | 0.910 | 0.353 |
| Shell density index $^{\Upsilon}$ | **< 0.002** | **< 0.005** | **< 0.001** | 1 | 1 | 1 |

$^{\Upsilon}$ Pairwise comparisons using t-test (Welch)

**Table 3** Summary of statistics **A**. Nested ANOVA results of the effects of pH on shell fracture force in juvenile *H. tuberculata* (pH: fixed factor, tank: random factor nested into pH). **B.** Multiple comparison Tukey's HSD Test testing the influence of decreased pH on shell fracture force in juvenile abalone *H. tuberculata*. Significant *P*-values in bold ($P < 0.05$).

**A.**

| | SS | df | MS | *F*-ratio | *P*-value |
|---|---|---|---|---|---|
| pH | 101.55 | 3 | 33.85 | 11.15 | **0.0047** |
| Residuals | 21.26 | 7 | 3.04 | | |
| Error (tank) | 81.08 | 31 | 2.615 | | |

**B.**

| pH groups | Estimate | SE | df | *t*-ratio | *P*-value |
|---|---|---|---|---|---|
| 7.6/7.7 | -4.0269558 | 0.8592177 | 7 | -4.687 | **0.0093** |
| 7.6/7.8 | -4.4608812 | 0.8483779 | 7 | -5.258 | **0.0050** |
| 7.6/8.1 | -3.8520031 | 0.8503777 | 7 | -4.530 | **0.0112** |
| 7.7/7.8 | -0.4339255 | 0.7473146 | 7 | -0.581 | 0.9348 |
| 7.7/7.8 | 0.1749527 | 0.7495841 | 7 | 0.233 | 0.9951 |
| 7.8/8.1 | 0.6088781 | 0.7371338 | 7 | 0.826 | 0.8407 |

**Table 4** Summary of the linear model testing the effects of decreased pH, weight and the interaction pH * weight on the shell fracture force. Significant *P*-values in bold ($P < 0.05$).

| Source | SS | df | MS | *F*-ratio | *P*-value |
|---|---|---|---|---|---|
| pH | 11.476 | 3 | 3.825 | 2.017 | 0.13 |
| Weight | 125.154 | 1 | 125.154 | 65.967 | **$<10^{-8}$** |
| pH * Weight | 2.764 | 3 | 0.921 | 0.486 | 0.69 |
| Residuals | 64.496 | 34 | 1.897 | | |